MATHEMATICAL MODELLING OF HYBRID POWERTRAIN SYSTEMS FOR IMPROVED ENERGY EFFICIENCY

Oleg Lyashuk[1,*], Victor Aulin[2], Roman Rohatynskiy[1], Ivan Gevko[1], Andriy Gypka[1], Dmytro Mironov[1], Volodymyr Martyniuk[3,4], Artur Lutsyk[1], Nadia Denysiuk[5]

[1]Department of Automobiles, Ternopil Ivan Puluj National Technical University, Ternopil, Ukraine
[2]Department of Maintenance and Repair of Machines, Central Ukrainian National Technical University, Kirovohrad, Ukraine
[3]Administration and Social Sciences Faculty, WSEI University, Lublin, Poland
[4]Administrative and Financial Management Department, Lviv Polytechnic National University, Lviv, Ukraine
[5]Department of Ukrainian and Foreign Languages, Ternopil Ivan Puluj National Technical University, Ternopil, Ukraine

*E-mail of corresponding author: oleglashuk@ukr.net

Oleg Lyashuk 0000-0003-4881-8568,
Roman Rohatynskiy 0000-0001-8536-4599,
Andriy Gypka 0000-0002-7565-5664,
Volodymyr Martyniuk 0000-0003-4139-0554,
Nadia Denysiuk 0000-0001-8197-2183
Victor Aulin 0000-0002-9658-2492,
Ivan Gevko 0000-0001-5170-0857,
Dmytro Mironov 0000-0002-5717-4322,
Artur Lutsyk 0009-0003-3938-9228,

Resume
The development and simulation of a mathematical model for a hybrid powertrain vehicle, aiming to optimize its energy efficiency and dynamic performance is presented in this study. Implemented in MATLAB/Simulink, the model captures the dynamic interactions between the hybrid system's components, including the internal combustion engine, electric motor, and battery. By conducting a full factorial experiment, the specific power of the hybrid vehicle was analyzed, revealing the critical influence of factors such as driving speed, road gradient, and battery state of charge. The proposed model demonstrated a discrepancy of 4-11% between the simulated and experimental results, confirming its adequacy for forecasting energy consumption and operational range. These findings offer valuable insights for enhancing the hybrid vehicle performance and sustainability through precise energy management strategies.

Article info
Received 30 September 2024
Accepted 27 February 2025
Online 19 March 2025

Keywords:
hybrid power plant
drive
electric motor
transmission
generator
car

Available online: https://doi.org/10.26552/com.C.2025.028

ISSN 1335-4205 (print version)
ISSN 2585-7878 (online version)

1 Introduction

Recent years have been characterized by high growth rates of the global automobile fleet, causing the increase in oil consumption and emissions of harmful substances with exhaust gases. Improving the fuel efficiency and reducing emissions is a priority in the design of automobiles. These problems can be solved by the improvement of the design of internal combustion engines (ICE), the use of alternative fuels (biofuels, natural gas, etc.) [1-2], and the increase in the energy efficiency of automobiles. The use of electric and hybrid power plants (HPP) in road transport is particularly noteworthy.

The production of hybrid buses is a global trend in the bus industry. Many global manufacturers, in particular North American ones, most actively participate in the development of hybrid power plants and buses in cooperation with major energy companies and national laboratories such as EPRI, General Electric, NREL, INEEL, ISE Research, and others. Design and production are carried out in accordance with the government program "The 21st Century Truck Program (21CT)" and the program of US Department of Energy (DOE) "Advanced Heavy Vehicle Hybrid Propulsion System R&D Program (Heavy Hybrid Program)". In 2002, at the request of the US Department of Energy, the NREL National Laboratory analyzed the development of hybrid trucks and buses of various types in order to determine the concept of designing hybrid

power plants for urban and suburban transport. In this study [3], the authors analysed the optimisation of timetables and scheduling for electric buses. They proposed a new approach that combines scheduling and traffic planning to improve service quality and reduce operating costs. Using the case of a university bus route in Montreal, the authors developed a mathematical model and algorithm that takes into account passenger waiting time and seat availability. As a result, the proposed approach significantly improved service and reduced costs compared to the existing schedule.

Keseev (2023) [4] conducted a comprehensive gap analysis in the classification of eco-friendly vehicle categories, emphasizing the environmental and economic benefits of hybrid electric vehicles (HEVs) and plug-in hybrid electric vehicles (PHEVs) over the battery electric vehicles (BEVs) for diverse driving conditions. The findings highlight that HEVs and PHEVs are more versatile and economically viable, especially in urban and extra-urban environments, whereas BEVs are mainly effective in city driving due to infrastructure and battery limitations. However, this research did not extensively address the modelling and simulation of hybrid powertrain systems to optimize performance parameters such as energy consumption and vehicle dynamics. This gap underlines the need for advanced mathematical models to enhance hybrid vehicle efficiency.

The authors of this study [5] offered a detailed analysis of the sizing of powertrain components in commercially available electrified vehicles, focusing on internal combustion engines, electric motors, and battery capacities across HEV, PHEV, and BEV models. The research identified how the powertrain components are dimensioned to meet specific performance requirements, such as acceleration and driving range, using data-driven methodologies. However, the static sizing approaches, without exploring dynamic simulation or optimization of powertrain operations under varying driving conditions were primarily emphasized in this study. This gap highlights the need for comprehensive modelling that incorporates dynamic performance and energy management strategies.

In the study [6] authors investigated the power loss analysis of semiconductor devices in multi-phase traction inverter topologies for automotive applications. The research compared traditional two-level Voltage Source Inverters (VSI) to advanced three-level Neutral Point Clamped (NPC) and T-type NPC (T-NPC) inverters, using PLECS and MATLAB simulations. The findings demonstrate that T-NPC inverters offer superior efficiency and reduced power losses, particularly at higher switching frequencies. However, authors primarily focuse on inverter topology optimization without addressing how these advancements impact the overall energy management and dynamic performance of hybrid powertrains. This limitation underscores the need for integrated modelling of hybrid vehicle systems.

The authors of this study note that the introduction of the HPP will significantly improve the environmental and economic performance of a vehicle. The papers [7-11] provide a justification for the need to create vehicles for urban passenger transportation with a hybrid power plant. The authors underline that combining the positive qualities of an internal combustion engine and a traction electric drive of a vehicle allows obtaining advantages over a traditional design by increasing environmental friendliness, cutting fuel consumption, improving dynamic properties, and increasing the efficiency of the power plant. In [12], the authors analyzed current innovations in electric vehicles (EVs) for the energy transition. They emphasised the importance of EVs in reducing dependence on fossil fuels and reducing carbon dioxide emissions. The latest technologies, market trends and challenges related to the development of EFVs, as well as prospects for future development were covered in this study. The main focus was on technological improvements, the expansion of charging infrastructure and policy support required for the widespread adoption of EVs.

The system “HPP - automobile - road” is considered in [13]. This approach requires the development of models for each component of the system. Currently, there are various models of HPP, the automobile, and the road. Specific method was applied for designing models that describe the dynamics of automobile movement, design features, and road conditions [14]. However, the generalizing features among the HPP models could not be distinguished; thus, the assessment of indicators by this method is ambiguous. In [15], the authors analyzed the use of hybrid reinforcement learning models to optimise the charging and discharging of lithium-ion batteries in electric vehicles. They integrated the deep Q-learning and active criticism algorithms into the battery management systems. This improves the battery efficiency, performance and service life. The models have been tested in simulations and experimental environments, demonstrating the ability to adapt to changes in battery health and adhere to complex operational constraints.

When studying the performances of automobiles with HPP [16], the maximum power was assumed decisive for determining the choice of series or parallel HPP layout scheme. The parallel one was assumed suitable for power up to 150 kW, typically for passenger cars. The series scheme was assumed suitable for power plant capacities greater than 150 kW, such as heavy-duty vehicles. The choice based on power is not used today. As technology is constantly evolving, the usefulness of a series or parallel scheme has become less significant with the advent of mixed control algorithms for HPP. Therefore, all the processes and traction-and-speed properties of vehicles could be better optimized. Based on the above, the rational parameters of the hybrid power plant should be selected for the automobiles of M3 category with consideration of the

control algorithm, provided the required indicators of specific power consumption of the hybrid vehicle be ensured.

2 Materials and methods

A vehicle with HPP is a complex mechatronic system with coordinated operation of electrical, mechanical, and thermal units. When modelling a vehicle with HPP, the simulation of the control object and the control algorithm should be carried out in a single environment. Such simulation allows optimizing the entire system. To provide effective modelling, a balance between calculation accuracy and modelling speed should be maintained. To quickly execute the model, fast iterations, i.e., not very accurate, are required at some stages of development. There are several approaches to modelling.

One of them is the modelling from the power plant (PP) to the drive of the drive wheels (DDW) [17-18]. The principle of modelling from PP to DDW is shown schematically in Figure 1.

This method is used in cases when there is a need to quickly execute the model with a small number of simulation iterations and their low accuracy. Although this method minimizes the number of options for model calculations, it contains a number of uncertainties regarding the input parameters, which can critically affect the accuracy of the calculations.

The method of modelling from DDW to PP is more rational (Figure 2), as the operating conditions are known at the initial stage of the design. Therefore, the general requirements for electrical, mechanical, thermal units, and the control system of the car's power plant could be substantiated; the energy and technical and economic indicators of the unit could also be predicted.

Having specified the operating mode (i. e., in the form of a change in the speed of the car over time and the dynamic radius of the wheel), the power, torque and angular velocity could be determined and then created on DDW shaft. Therefore, having specified the efficiency value of the transmission, the moment of shafts inertia, the transmission ratio (or a series of transmission ratios) of DDW, the power, torque and rotation frequency, created by the automobile PP, are determined. Then, having accepted the previous values of the PP efficiency, the power provided by PP could be determined. The obtained power value of PP allows choosing the optimal power distribution parameters between the PP units to meet the given operating mode. This approach to designing automobiles with HPP is methodologically more justified. It allows selecting and substantiating the values of the maximum power of the power plant, the distribution of power between the internal combustion engine and the electric motor, the amount of energy required for the driving cycle, the capacity and power of the battery, and fuel consumption. It is also possible to select optimal conditions for the transition between states (modes) of the power plant. In addition, it allows minimizing the number of calculation options and eliminating a number of uncertainties that complicate the design process. That is why this approach was chosen to implement the mathematical model of the hybrid.

In this paper, the principle of modelling a hybrid car with a sequential power plant configuration is considered. A hybrid car with a serial configuration scheme is structurally simpler (and therefore simpler from the point of view of modelling its operation) than a hybrid car with a parallel scheme, since only an electric motor is used as a driving component. The structural scheme of an automobile with HPP, which has the main functional elements and input/output signals of each of them, is considered in the paper (Figure 3).

The main functional elements are the automobile rechargeable battery (BAT), the drive of driving wheels (DDW) of a rear axle, the internal combustion engine (ICE), the motor/generator (M/G), the gearbox (GC), rear drive wheels (WL), the GC control unit (GCU) and automatic control system (ACS). The latter combines the control logic (CL) and control circuits for the internal combustion engine and electric motor, which consist of

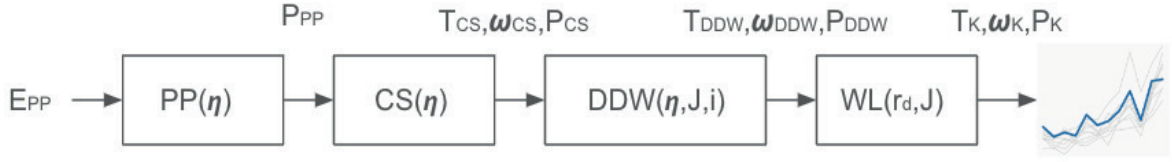

Figure 1 *Structural scheme of an automobile with HPP modelled from PP to DDW*

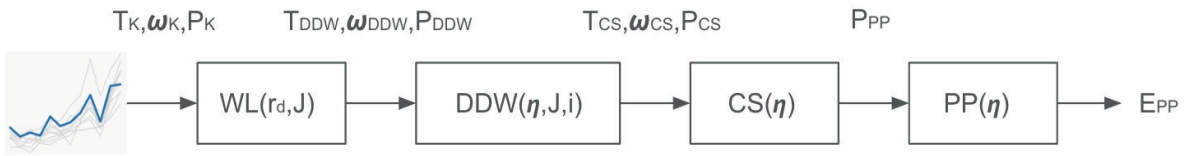

Figure 2 *Structural scheme of an automobile with HPP modelled from DDW to PP*

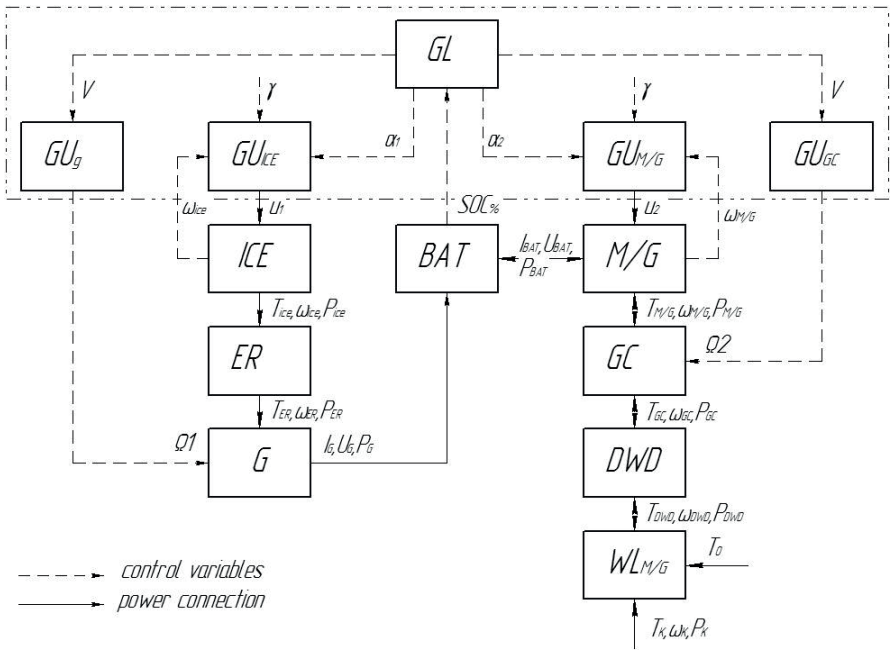

Figure 3 *Considered structural scheme of an automobile with HPP*

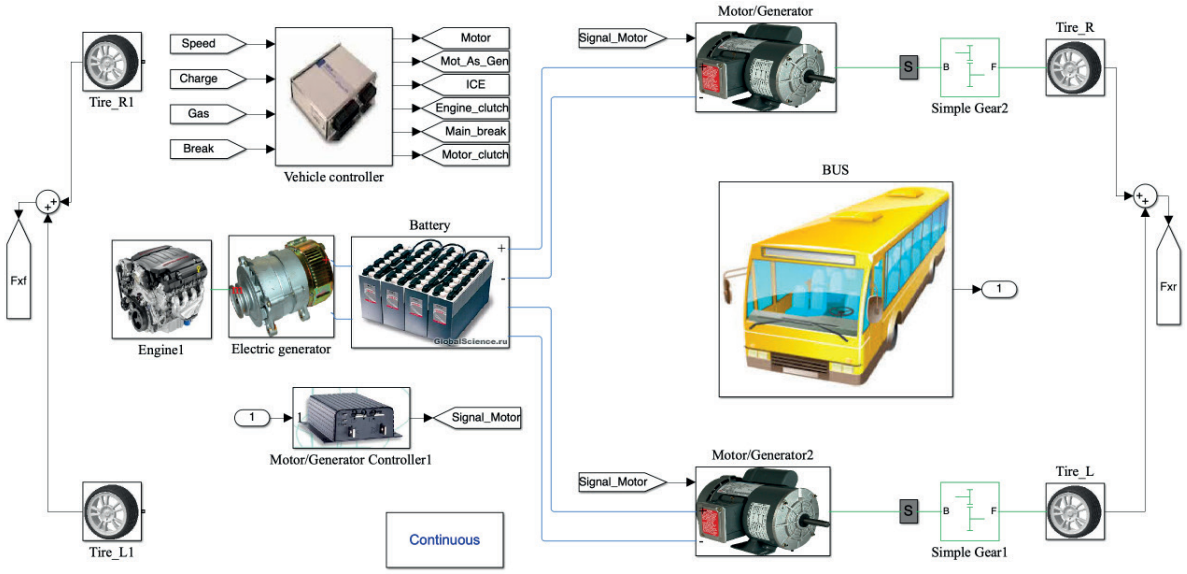

Figure 4 *Simulink model of an automobile with HPP of a serial type*

the control unit *ICE-CU*$_{ICE}$ and the electric motor control unit - $CU_{M/G}$.

The control logic forms the control signals α_1, α_2, which are sent to the CU_{ICE} and $CU_{M/G}$; the output signals of the latter are u_1 and u_2, which represent the control action on the ICE and M/G

The power of the battery P_{BAT}, which is proportional to the voltage U_{BAT} and the current I_{BAT}, ensures the operation of the M/G in traction mode. When working in the traction mode, M/G creates mechanical power $P_{M/G}$, which is proportional to torque $T_{M/G}$ and angular velocity $\omega_{M/G}$, and is transmitted to DDW. The power on the driving wheels P_{WL} is determined by the power P_{DDW}, which, in turn, depends on the current value of the torque of the drive of the driving motor T_{DDM}, the angular velocity P_{DDM}, and the moment of the resistance forces T_o. In the braking mode, the M/G converts the mechanical energy from the DDW into electrical energy and charges the battery.

The ICE is used exclusively to recharge the batteries. When operating, the ICE generates mechanical power P_{ICE}, which is proportional to the torque T_{ICE} and angular velocity P_{ICE}, and is transmitted to the generator G. The power at the generator is determined by the power of the engine reducer P_{ER}, which, in turn, depends on the current value of the torque T_{ER}, the angular velocity $\omega_{ER,}$ and the moment of resistance forces T_O. The generated energy is supplied from the generator to the battery.

To model an automobile with HPP, a control

algorithm was considered using the MatLab Simulink environment. In accordance with the structural scheme of the vehicle with HPP, the mathematical model is presented in Figure 4. The mathematical model was developed using the current recommendations [19-20].

The mathematical model of a car with a sequential type HPP consists of the main blocks: Engine - diesel engine model; MG - model of electric motor /generator; Battery - battery model; Front Transmission - front beam model; Rear Transmission - rear axle model; Longitudinal Vehicle Dynamics - model of a longitudinal dynamics of vehicle movement; Wheel - four blocks that model the wheels of the car; Vehicle controller - model of the vehicle operating mode control system; Engine Controller - model of the diesel engine control unit; MG Controller - model of the electric motor - generator control unit.

When developing a mathematical model that describes the dynamics of a vehicle with HPP in various modes of power plant operation, the elastic and deformable properties of the transmission, as well as possible slippage of the drive wheels when the vehicle is moving, were not taken into account. When modelling the internal combustion engine, thermodynamic processes were not taken into account, as well. The battery capacity with a maximum permissible discharge of 70% of the total capacity was assumed sufficient to complete the driving cycle. Additionally, the model set the parameters of the road surface. The road was chosen to be flat and straight. The longitudinal slope of the road was set to +5%. The maximum transverse curvature of the road was 1.5%. The test cycle for modelling was the European urban driving cycle ECE 15 [21], lasting 195 s.

A model of a petrol engine with angular velocity control is under study in this paper. The input parameter of the ICE model is the throttle valve opening. The parameters that define the engine model are maximum power, angular velocity at maximum power, and maximum angular velocity of the crankshaft.

Current angular velocity value ω_i is a feedback to the motor model input. The angular speed of the motor is limited: $\omega_{\min} \le \omega_i \le \omega_{\max}$. The maximum engine power $P_{\max}$ corresponds to ω_P thus, $P_{\max} = f(\omega_P)$. The equation that determines the maximum torque [17]:

$$T_{\max} = \frac{P_{\max}}{\max}. \tag{1}$$

A well-known relationship is used to describe the dependence of the power of an internal combustion engine on the angular velocity of the crankshaft:

$$P(\omega) = P_{\max}\left[p_1\frac{\omega_i}{\omega_N} + p_2\left(\frac{\omega_i}{\omega_N}\right)^2 + p_3\left(\frac{\omega_i}{\omega_N}\right)^3\right], \tag{2}$$

where p_1, p_2, p_3 - Leiderman coefficients; ω_N - the nominal (rated) angular velocity of the crankshaft

The electric motor model is a model of a brush motor with torque feedback control [13]. This block represents the dependence of torque on angular velocity $T_m(\omega_m)$. Applying a well-known relation, the dependence $T_m(\omega_m)$ is converted into a voltage and current dependence $U_m(I_m)$:

$$\begin{cases} I_m = T_m/(k\Phi_m) \\ E_m = k\omega_m\Phi_m \\ U_m = E_m + I_m\sum R_m \end{cases}, \tag{3}$$

where k - motor design factor; Φ_m - magnetic flux; R_m - resistance; E_m- electromotive force (EMF); $\sum R_m$ - total winding resistance.

The model ensures the output of a certain torque at a certain speed, the values of which are predefined, when the block parameters are set.

The battery model is a dynamic model of the parameters of a lithium-ion battery [17]. The model is divided into two main components - the charge model and the discharge model.

Discharge model $i^* > 0$:

$$f_1(it, i^*, i) = U_0 - K\cdot\frac{Q}{Q-it}\cdot i^* - \\ -K\cdot\frac{Q}{Q-it}\cdot it + A\cdot\exp(-B\cdot it), \tag{4}$$

Charge model $i^* < 0$:

$$f_2(it, i^*, i) = U_0 - K\cdot\frac{Q}{it+0.1Q}\cdot i^* - \\ -K\cdot\frac{Q}{Q-it}\cdot it + A\cdot\exp(-B\cdot it), \tag{5}$$

where U_0 - rated EMF of the battery (V); K - polarization constant (A×H^{-1}) or polarization resistance (Ω); i*- low frequency dynamic current (A); i - battery current (A); it - instantaneous battery capacity (A×H); Q - maximum battery capacity (A×H); A - exponential voltage (V); B - exponential capacity (A×H).

The front axle DDW model (Figure 5) consists of the main blocks: Variable ratio transmission - gearbox unit; Gearboxlever - gearbox control system; Simple gear1 - block that simulates the main gear; Front differential - block that models the differential; Blocks that model the effect of the moment of mechanisms inertia.

The transmission unit is represented as a gearbox that dynamically transmits angular velocity and torque between the two axes, depending on the set gear ratio. If one ignores the change in angular velocity due to shaft stiffness and mechanical losses, the model can be represented by the equations:

$$\omega_B = u_{FB}(t)\omega_F, \tag{6}$$

$$T_F = u_{FB}(t)T_B, \tag{7}$$

where ω_B i ω_F - angular velocities of the input and output shafts, respectively; T_B and T_F - torque on the primary and secondary shafts, respectively; $u_{FB}(t)$ - gear ratio of the gearbox, which changes over time depending on driving conditions.

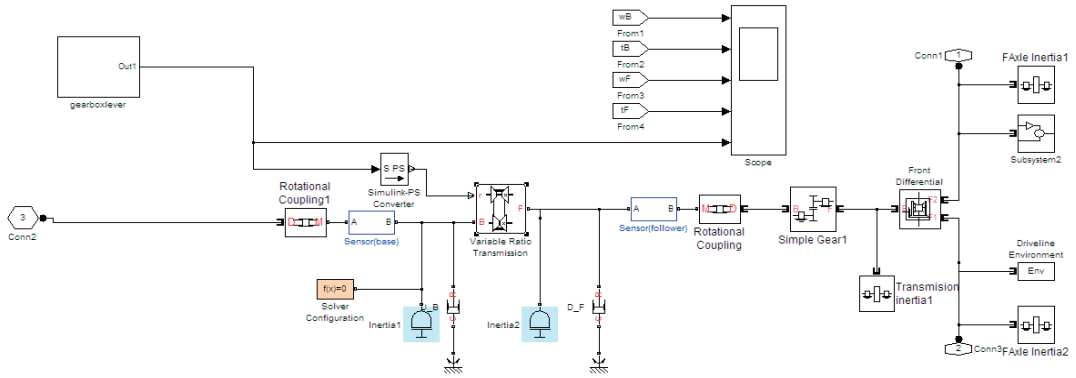

Figure 5 *Simulink front axle DDW model*

Based on the changes in angular velocity due to shaft torsion, the instantaneous change in time between angular velocities over time is calculated as

$$d\phi/dt = u_{FB}(t)\omega_F - \omega_B, \tag{8}$$

where ϕ - shaft twist angle.

The torque is determined as:

$$T_B = -k_P - k_V d\phi/dt, \tag{9}$$

where k_p and k_V - empirical coefficients.

The torque loss in the box is calculated using the formula:

$$T_{loos} = T_F(1-\eta_g), \tag{10}$$

where η_g - gearbox efficiency.

Taking into account mechanical losses, the resulting model is developed:

$$u_{FB}(t)T_B - T_F - T_{loss} = 0. \tag{11}$$

The control system is modelled to evaluate and optimize the interaction between the various components of the hybrid, such as the internal combustion engine (ICE), electric motor and traction battery. The control system model is integrated into a general model of a vehicle with a sequential type of HPP. The control object and control algorithm are modelled in a single Stateflow environment, which is used to model and simulate combinatorial and sequential decision-making logic based on machine states and flowcharts. The Vehicle controller is a sequential control unit based on the theory of finite state machines. The proposed model uses a deterministic finite state machine Q, which is represented by five components:

$$Q = f(S, \Sigma, \delta_i, s_0, R), \tag{12}$$

where S - set of states; Σ - set of input characters; δ_i - transition function; s_0 - initial state; R - set of final states.

The arguments of the transition function δ_i are the current state and the input signal, and the value is the new state. If s is the state and λ is the input state, then $\delta_i(s,\lambda)$ - is the state p.

The control logic model has two main states, one of which has two sub-states, and the other has three sub-states, two of which also have two sub-states. The formula is deduced:

$$Q = \begin{bmatrix} s_1(s_{11}, s_{12}\{s_{121}, s_{122}\}), \\ s_2(s_{21}, s_{22}\{s_{221}, s_{222}\}), \\ c_1(j_1, j_2, j_3, j_4\{r_1, r_2\}), \\ c_2(i_1, i_2, i_3, i_4\{l_1, l_2\}), \\ \delta_i, \\ s_{21}, \end{bmatrix} \tag{13}$$

where s_1, s_2 - main states; s_{11}, s_{12} - sub-states of the main state s_1; s_{121}, s_{122} - sub-states of state s_{12}; s_{21}, s_{22}, s_{23} - sub-states of the main state s_2; s_{221}, s_{222} - sub-states of state s_{22}; c_1 - condition of transition from state s_1 to state s_2; c_2 - condition of transition from state s_2 to state s_1; j_1 - condition of entry into state s_{11}; j_2 - condition of entry into state s_{12}; j_3 - condition of transition from state s_{11} to s_{12}; j_4 - condition of transition from state s_{12} to s_{11}; r_1 - condition of transition from state s_{121} to s_{122}; r_2 - condition of transition from state s_{122} to s_{121}; i_1 - condition of entry into state s_{21}; i_2 - condition of entry into state s_{22}; i_3 - condition of transition from state s_{21} to s_{22}; i_4 - condition of transition from state s_{22} to s_{21}; l_1 - condition of transition from state s_{221} to s_{222}; l_2 - condition of transition from state s_{222} to s_{221}.

Based on Moore's model, the logic is described:

$$\begin{aligned} &s_1, c_1 \mapsto s_2; s_2, c_2 \mapsto s_1; \\ &s_{11}, j_1 \mapsto s_{11}; s_{11}, j_3 \mapsto s_{12}; s_{12}, j_2 \mapsto s_{12}; s_{12}, j_4 \mapsto s_{11}; \\ &s_{121}, r_1 \mapsto s_{122}; s_{122}, r_2 \mapsto s_{121}; \\ &s_{21}, i_1 \mapsto s_{21}; s_{21}, i_3 \mapsto s_{22}; s_{22}, i_2 \mapsto s_{22}; s_{22}, i_4 \mapsto s_{21}; \\ &s_{221}, l_1 \mapsto s_{222}; s_{222}, l_2 \mapsto s_{221}. \end{aligned} \tag{14}$$

The control logic is implemented using the Stateflow tool in the MatLab Simulink environment. Figure 6 shows a block diagram of the control algorithm.

The implemented control algorithm should be further considered. Figure 7 shows

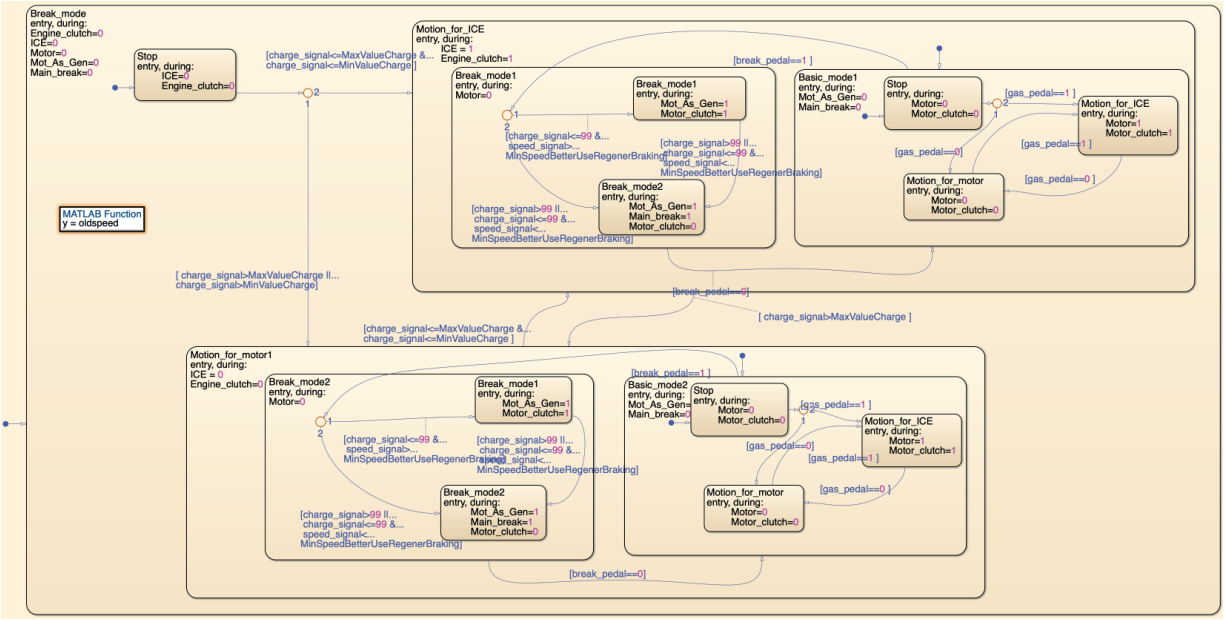

Figure 6 *Block diagram of the algorithm for controlling the power plant of an automobile with HPP*

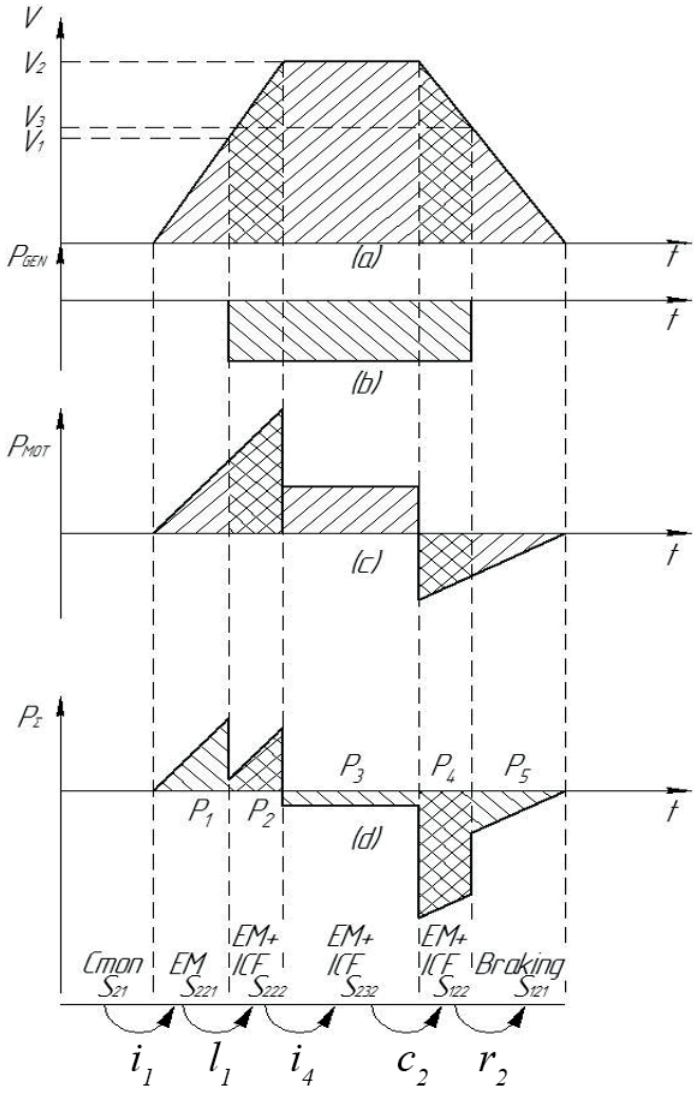

Figure 7 *Scheme of movement modes and transition conditions when an automobile with HPP is moving: a) dependence of automobile speed on time; b) dependence of the power generated by the generator on time; c) dependence of required power for automobile speed mode on time; d) dependence of total power consumed by an automobile on time*

a diagram of the movement modes and transition conditions when an automobile with HPP is moving.

The accepted notation is used in the MatLab Simulink environment. Input signals: gas - accelerator pedal signal (1, 0); break - brake pedal signal (1, 0); Charge - signal about the amount of battery power; Speed - vehicle speed; Output signals: Motor - the electric motor drives the wheels of the vehicle and charges the battery during regenerative braking (on/off) → (1, 0); Mot_As_Gen - electric motor in generator mode for regenerative braking, (on/off) → (1, 0); ICE - internal combustion engine, (on/off) → (1, 0); Engine_clutch - internal combustion engine clutch, (on/off) → (1, 0); Main_break - service brake system (on/off) → (1, 0); Motor_clutch - clutch of the electric motor to the wheel drive, (on/off) → (1, 0).

The basic control logic of a power plant of an automobile with HPP of a serial type has two main modes: (s_2) - basic mode (movement with ICE running) (Figure 8), (s_1) - additional mode (movement with ICE off) (Figure 9). The transition from mode (s_2) to mode (s_1) is carried out when the condition (c_1) is met, which indicates that the battery charge has reached a certain value. The transition from mode (s_1) to mode (s_2) is carried out when the condition (c_2) is met, which indicates that the battery discharge is below the minimum permissible value. The block diagram of the control algorithm in the additional mode (s_1) is shown in Figure 7, where the parking mode occurs; the process of steady or accelerated movement of a vehicle is controlled; and braking with a regenerative braking system takes place.

The transition to the additional mode occurs when the battery is charged to 100%, if the conditions (c_1) is met, from any mode. In this mode, the internal combustion engine and, accordingly, the generator, are turned off. In this mode, the logic can be considered in two ways.

The fulfilment of conditions (r_1) or (r_2) indicates that the brake pedal is pressed, and the driving speed is greater than the minimum permissible value, from which it is advisable to start regenerative braking (the speed is calculated depending on the driving cycle for each automobile specifically). There is a transition to mode (s_{121}) or (s_{221}), respectively, in which the operation of the motor/generator in engine mode is stopped and regenerative braking is activated.

Based on the developed model of hybrid car control, the simulation modelling of the hybrid's operation was performed. The simulation results for the main components of the hybrid (internal combustion engine, traction battery, and electric motor) are shown in Figures 10-12.

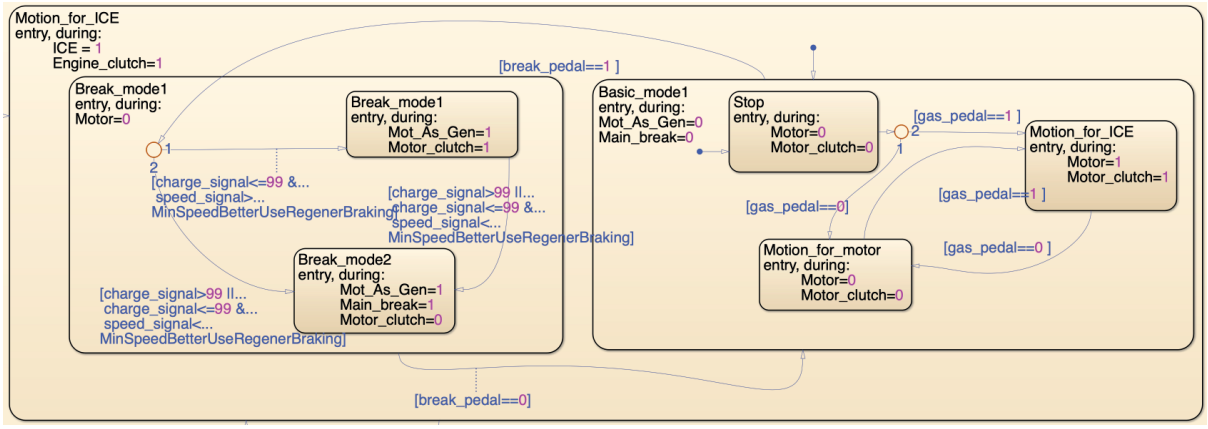

Figure 8 *Block diagram of the control algorithm in the main mode*

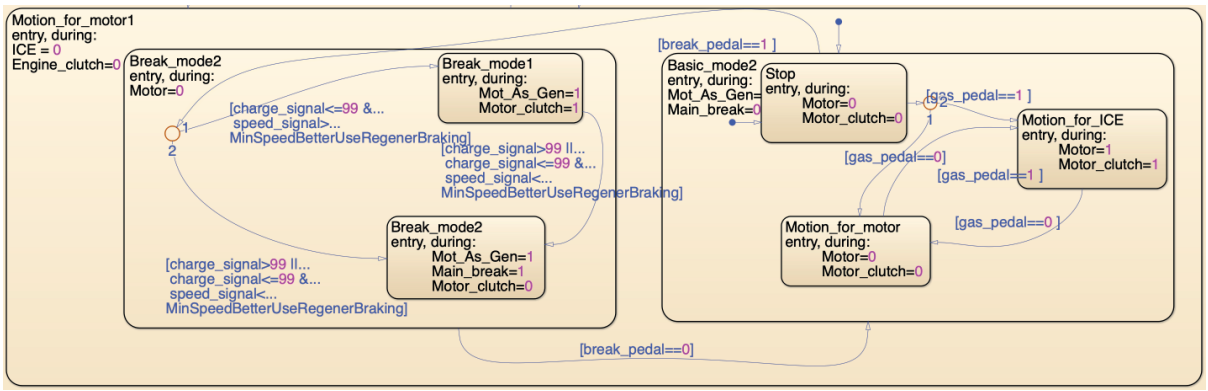

Figure 9 *Block diagram of the control algorithm in additional mode*

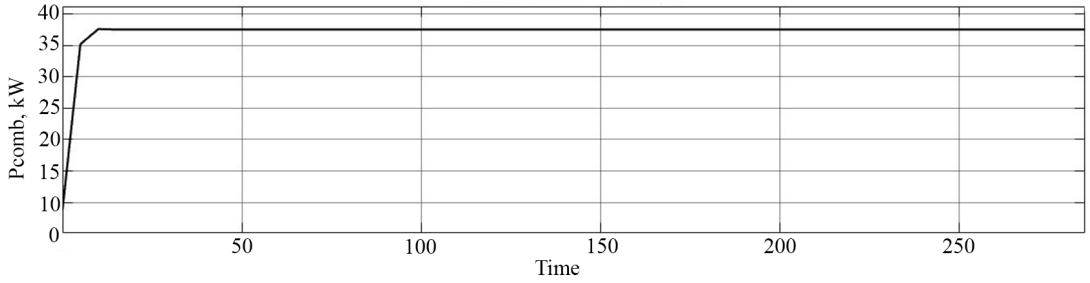

Figure 10 *Power of an internal combustion engine according to simulation in the Simulink environment*

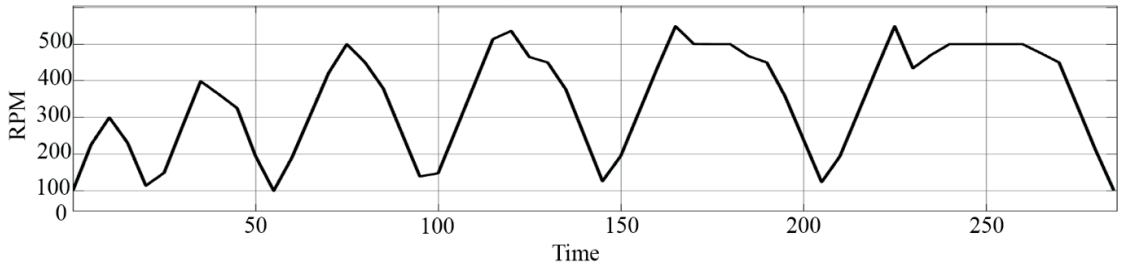

Figure 11 *Electric motor speed according to simulation in the Simulink environment*

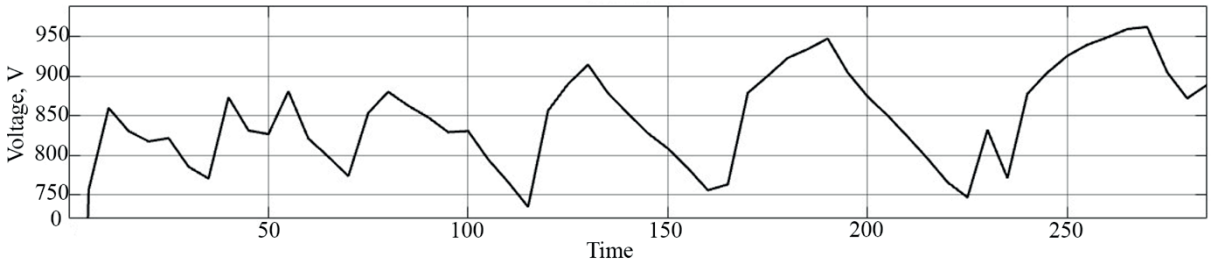

Figure 12 *Battery voltage according to simulation in the Simulink environment*

The graph in Figure 10 shows the power output of an internal combustion engine (ICE) at different points in time during a Simulink simulation. The visible power fluctuations reflect the different modes of the vehicle operation, including acceleration and steady state driving. This data helps to assess the efficiency of the engine in different driving conditions.

The graph in Figure 11 illustrates the changes in motor speed during the simulation. The speed changes according to the different driving modes of a vehicle, including acceleration, steady-state driving, and regenerative braking. This information is key to understanding the efficiency of the motor in different operating conditions.

The graph in Figure 12 shows the change in the voltage across the battery (during the simulation). The voltage fluctuates depending on the processes of charging and discharging the battery that occur during different modes of operation of a hybrid vehicle.

Additionally, the model of the hybrid vehicle control algorithm, proposed in this paper, was compared to the models of the control algorithms based on fuzzy logic [3, 7]. To test the effect of the two control algorithms on the energy characteristics of a hybrid vehicle, a road slope of 5% was set. The comparison was performed for three different modes of hybrid operation: electric motor operation, operation from a combination of an electric motor and an internal combustion engine, and operation from an internal combustion engine. Table 1 shows the results of modelling the operation of a hybrid vehicle using the developed control algorithm and the control algorithm based on fuzzy logic.

As shown in Table 1, when the hybrid vehicle is operating in the ”By EM” mode, the developed algorithm provides a 6% higher maximum engine power and a 5% higher electric motor speed compared to the fuzzy logic-based algorithm. The voltage also increases by an average of 4.5%, indicating the better energy efficiency and stability.

Similar results were obtained in the “By EM and ICE” mode - here, the developed algorithm provides a wider range of engine power, with a maximum value of 6% higher. The voltage increases by an average of 3.4%, and the motor speed increases by 6%. This results in more efficient energy use and better performance.

In the brake mode, the developed algorithm provides a 7% higher maximum motor power, a 4.6% higher voltage on average, and a 7% higher motor speed.

***Table 1** Energy characteristics of a hybrid vehicle*

No.	Driving modes	Developed algorithm	Algorithm based on fuzzy logic
		Internal combustion engine (kW)	
1	By EM	up to 262	up to 246
2	By EM and ICE	110	103
3	Brake mode	up to 175	up to 163
		Voltage (V)	
1	By EM	33.1	31.6
2	By EM and ICE	34.5	33.3
3	Brake mode	41.5	39.5
		Electric motor speed (RPM)	
1	By EM	9.8	9.3
2	By ICE	3.4	3.2
3	By EM and ICE	2.8	2.6

This indicates the better energy efficiency and energy recovery during braking.

A comparative analysis of the two strategies for controlling the torque distribution shows that the developed hybrid vehicle control algorithm outperforms the fuzzy logic-based algorithm in all the analyzed driving modes. It provides higher motor power, higher voltage, and higher electric motor speed. This indicates a higher energy efficiency and stability of the hybrid vehicle under the control of the developed algorithm compared to the fuzzy logic-based algorithm.

An equally important parameter of a hybrid vehicle's operation is the specific power [22]. Evaluating and optimizing the factors that influence the specific power of a hybrid vehicle is important from the perspective of hybrid vehicle performance, as it affects the acceleration and overall dynamic performance of a vehicle, as well as its overall efficiency and economy. To assess the factors that influence the specific power of a hybrid, a regression mathematical model of the vehicle specific power was developed. To form the regression model, the method of planning a multivariate experiment was applied.

When developing an experiment plan, optimality criteria and scope of research come to the fore. In this context, it becomes clear that the optimal plan should be two-level (since the emphasis is on the linear model), with orthogonality and the possibility of rotation. At the first stage of conducting a full factorial experiment, the selection of factors and response functions and the area of their definition is performed [23]:

$$\begin{aligned} y_{\min} \le y \le y_{\max}, \\ x_{\min} \le x \le x_{\max}. \end{aligned} \tag{15}$$

To simplify the recording of experimental conditions and the processing of experimental data, the coding of factors is performed. For this purpose, zero levels for each factor x_{io} and intervals of their variation x_i are selected in the field of determining factors. The upper x_{ib} and lower x_{in} factor levels are calculated in natural values [23]:

$$\begin{aligned} x_{ib} = x_{io} + x_i, \\ x_{ib} = x_{io} - x_i. \end{aligned} \tag{16}$$

Then, the transition to the dimensionless coordinate system is performed:

$$x_j = \frac{K_j \tilde{x}_j - K_{jo} \tilde{x}_{jo}}{I_j}, \tag{17}$$

where x_j - coded value of the factor, $K_j \tilde{x}_j$ - natural value of the factor, $K_{jo} \tilde{x}_{jo}$ - natural value of the main level, I_j - variation interval, j - number of the factor. For quality factors with two levels, one level is +1, and the other is - 1, the order of the levels does not matter.

The next step is to develop an experiment-planning matrix by recording the coded values of the factors and the resulting response function for each experiment. A complete factorial experiment implements all the unique combinations of levels of n independent variables, each of which varies at two levels. The number of such combinations is $N = 2^n$, if n is the number of factors. The developed experiment-planning matrix must satisfy the requirements [24]:

1) Symmetry relative to the center of the experiment

$$\sum_{i=1}^{N} x_{ji} = 0, \tag{18}$$

where j - number of the factor, N - number of experiments, j = 1,2,.....k.

2) Rationing condition

$$\sum_{i=1}^{N} x_{ji}^2 = N. \tag{19}$$

This is a consequence of the fact that the values of the factors in the matrix are set +1 and -1.

3) Orthogonality of the planning matrix

$$\sum_{i=1}^{N} x_{ji} \cdot x_{iu} = 0, \ j \ne u \ \ j = 0,1,2,.....,k. \tag{20}$$

4) Rotativity means that the points in the planning matrix are selected so that the accuracy of predicting

the values of the optimization parameter is the same at equal distances from the center of the experiment and does not depend on the direction.

In the resulting matrix of the experiment, the columns of controlled variables form the plan of the experiment. In addition, the full-factorial experiment (FFE) matrix includes a column with a fictitious factor x_o at the +1 level, which is needed to calculate the coefficient b_o of the regression equation [25]. The results of the experiment are recorded in the last column of the matrix. The response function in this case is the value Y, which takes the values $y_1, y_2, y_3,..., y_n$.

After conducting the FFE, the results are processed at the next stage [26]:

1) Calculation of the reproducibility variance estimation

$$S^2_{(y)} = \frac{\sum_1^N (y_i - \bar{y})^2}{N-1}, \quad (21)$$

where $\bar{y}$ - mathematical expectation of the response function, $N-1$ - the number of degrees of freedom.

2) Definition of regression coefficients

$$b_j = \frac{\sum_{i=1}^N y_i \cdot x_{ji}}{N}, \; b_0 = \bar{y}. \quad (22)$$

3) Checking the significance of regression coefficients.

$$S^2_{\{bj\}} = \frac{S^2_{\{y\}}}{N}, \; \Delta b_j = \pm t \cdot S_{\{bj\}}, \quad (23)$$

where t - tabular value of the Student's criterion for the number of degrees of freedom, at which $S2^2_{\{bj\}}$ was determined; and the selected level of significance (in this case, 0.05).

The coefficient is significant if its absolute value is greater than or equal to Δb_j. Additions with insignificant coefficients are excluded from the equation.

4) Testing the adequacy of the model.

$$F = \frac{S^2_{ad}}{S^2_{\{y\}}}, \quad (24)$$

where F - Fisher's criterion. Then, $F_{calcul} \langle F_{tabl}$; f - number of degrees of freedom, $f = N - (k+1)$; S^2_{ad} - variance of adequacy:

$$S^2_{ad} = \frac{\sum_{i=1}^N (y_i - \hat{y}_i)^2}{f}, \quad (25)$$

where $\hat{y}_i$ - value of the response function calculated by the regression equation; y_i - value of the response function obtained as a result of the experiment.

If a simple linear model turns out to be inadequate, additional methods are applied to improve adequacy: changing the limits of factor variation, shifting the center of the plan, or completing the experimental design. The latter approach involves the transition to orthogonal central compositional plans of higher order experiments.

3 Results and discussion

To obtain a mathematical model of the power change of a hybrid vehicle, a full factorial experiment was conducted. The specific power of the hybrid vehicle P was used as the response function. The main operational indicators and their change limits for obtaining P were determined (Table 2).

Based on the criteria of optimality and the number of factors, the plan of the full factorial experiment of the first order of type 2^4 was selected; and the planning matrix of the full factorial experiment was formed (Table 3), which consists of 16 experiments. The planning matrix contains the values of the factors in all the possible combinations. In the experiment matrix, the 2nd to 5th columns correspond to the factor values, the 6th column is the system response value, and the first column contains units corresponding to the unit coefficients of the free term of the model.

To unify the various physical factors and the response of the system, the transformation of dimensional physical values into dimensionless qualitative ones was performed using the Harington's desirability function [26].

Table 2 *Limits of changes in performance indicators*

Parameter	Moving speed, km/h	t of environment, C	Slope angle of the road surface, %	State of charge (SOC), %
Basic level	25	10	2.5	87.5
Variations	20	20	2.5	12.5
Upper level	45	30	5	100
Lower level	5	-10	0	75

Table 3 *Fragment of the planning matrix of a full factorial experiment*

Experiment number	x_0	x_1	x_2	x_3	x_4	P
1	1	0.780	0.421	0.780	0.765	0.665
2	1	0.780	0.390	0.780	0.765	0.663
3	1	0.375	0.421	0.780	0.765	0.554

Table 4 *Fragment of the coded planning matrix of a full factorial experiment*

Experiment number	1	2	3
x0	1	1	1
x1	1	1	-1
x2	1	-1	1
x3	1	1	1
x4	1	1	1
x1x2	1	-1	-1
x1x3	1	1	-1
x1x4	1	1	-1
x2x3	1	-1	1
x2x4	1	-1	1
x3x4	1	1	1
x1x2x3	1	-1	-1
x1x2x4	1	-1	-1
x1x3x4	1	1	-1
x2x3x4	1	-1	1
x1x2x3x4	1	-1	-1
P	0.665	0.653	0.554

Table 5 *Fragment of the coded planning matrix of the orthogonal central-composite plan of the second order*

Experiment number	1	2	3	4
x0	1	1	1	1
x1	1	1	-1	-1
x2	1	-1	1	-1
x3	1	1	1	1
x4	1	1	1	1
$x1^2$-α	0.2	0.2	0.2	0.2
$x2^2$-α	0.2	0.2	0.2	0.2
$x3^2$-α	0.2	0.2	0.2	0.2
$x4^2$-α	0.2	0.2	0.2	0.2
x1x2	1	-1	-1	1
x1x3	1	1	-1	-1
x1x4	1	1	-1	-1
x2x3	1	-1	1	-1
x2x4	1	-1	1	-1
x3x4	1	1	1	1
x1x2x3	1	-1	-1	1
x1x2x4	1	-1	-1	1
x1x3x4	1	1	-1	-1
x2x3x4	1	-1	1	-1
x1x2x3x4	1	-1	-1	1
P	0.665	0.653	0.554	0.544

At the next stage, to simplify the solution of the system, factors were normalized according to Equation (17). In addition, the planning matrix of the full factorial experiment is completed with rows of interaction of factors between themselves (rows 2-16) (Table 4).

The developed matrix satisfies the requirements in Equations (18)-(20). The specific power model of a hybrid vehicle, obtained because of a full factorial experiment, can be presented in the form of a general equation:

$$P = b_0 + b_1 \cdot x_1 + b_2 \cdot x_2 + b_3 \cdot x_3 + b_4 \cdot x_4 + \\ + b_5 \cdot x_1 \cdot x_2 + ... + b_{11} \cdot x_1 \cdot x_2 \cdot x_3 + \\ + b_{15} \cdot \cdot x_1 \cdot x_2 \cdot x_3 \cdot x_4. \quad (26)$$

The regression coefficients are determined according to Equation (22). The regression coefficients, whose value is equal to or greater than the confidence interval, are considered statistically significant and included in the final equation. As a result, the following regression equation was deduced:

$$P = 0.5104 + 0.0466 \cdot x_1 + 0.0588 \cdot x_2 + \\ + 0.0486 \cdot x_3 \quad . \quad (27)$$

The model was tested for adequacy by the Fisher's test according to Equation (24). The estimated value of Fisher's criterion F_{calcul} = 2.009633495, table F_{table} = 1.8874. Since the condition $F_{calcul} < F_{table}$ is not fulfilled, the model in Equation (27) cannot be considered adequate.

Based on the obtained results, it was decided to complete the plan of the full factorial experiment to the orthogonal central-compositional plan of the second order without losing information about the previous experiments (Table 5).

Analogous transformations with the planning matrix of the orthogonal central-composite plan of the second order allow obtaining the following regression equation:

$$P = 0.53476 + 0.0451 \cdot x_1 + 0.04368 \cdot x_3 + \\ + 0.03265 \cdot x_4 - 0.02975 \cdot x_2^2. \quad (28)$$

The model was tested for adequacy. The calculated value of the Fisher's criterion F_{calcul} = 1.632. For the given parameters of the experiment, F_{table} = 1.96. Based on the adequacy test, the model obtained is considered adequate (F_{calcul} = 0.0994 < F_{table} = 1.53).

Additionally, the model was tested by conducting experimental measurements with recording the values of statistically significant influence factors and the response function, and by calculating the value of the response function using a mathematical model. The object of the experimental study was a car with hybrid module (Figure 13).

The road tests were designed to verify the adequacy of the developed model in Equation (28) based on the conducted research and to refine it by accounting for factors present in real-world driving conditions. The testing program involved determining the kinematic and energy parameters of a hybrid-powered vehicle during straight-line motion under various driving modes with different energy sources. The tests were conducted in compliance with European standards EH 1986-2:2001 [27] and EH 1986-1 [28]. The testing equipment met the requirements of Directive 91/441/EEC. The test track was flat, straight, free of obstacles, and without wind barriers. The longitudinal slope of the test road did not exceed ±2%, while the maximum transverse curvature was limited to 1.5%. The driving cycle followed the European urban driving cycle ECE 15, with a total duration of 195 seconds.

The results of experimental measurements and

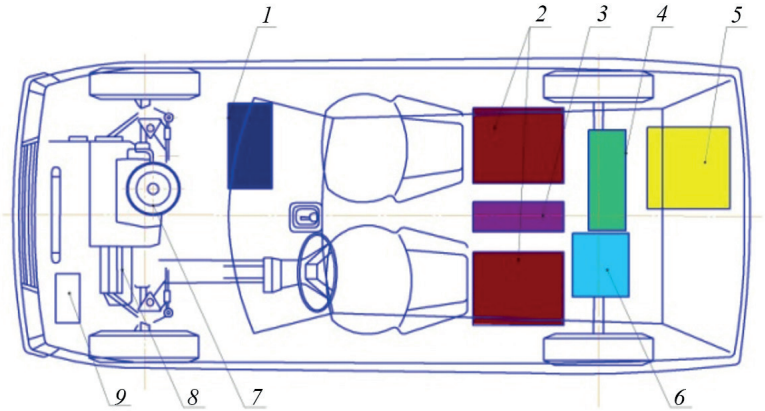

Figure 13 *Configuration of a vehicle with a hybrid powertrain system: 1 - control and data acquisition unit; 2 - traction battery pack (72 V); 3 - power converter unit; 4 - electric motor; 5 - fuel tank; 6 - rear axle transmission; 7 - internal combustion engine (ICE); 8 - front axle transmission; 9 - on-board battery (12 V)*

Table 6 *Fragment of the results of experimental measurements and modelling of the specific power of the hybrid*

Exp. No.	Moving speed, km/h	Ambient temperature, °C	Slope angle, %	SOC, %	Experimental Power, kW	Calculated Power, kW	Discrepancy, %
1	29.3	22.3	0.6	91.6	146.96	131.6	10.45
2	11.8	2.2	2.5	82.8	127.51	121.62	4.62
3	7.6	-6.1	0.2	88.0	143.95	136.22	5.37
4	43.0	17.4	4.5	88.7	139.48	133.46	4.32
5	43.6	7.6	1.3	79.6	109.79	102.9	6.28

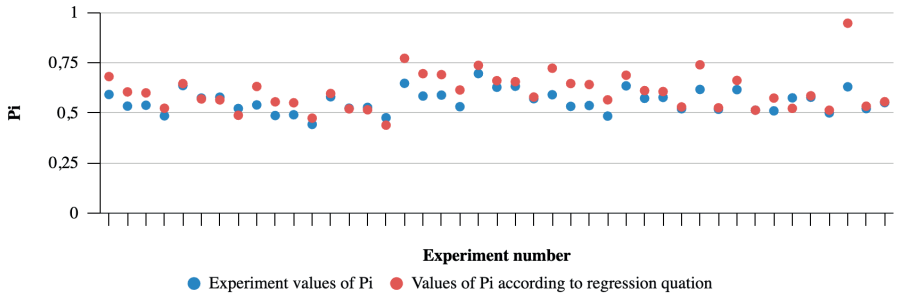

Figure 14 *Specific power of a hybrid vehicle according to the experiment data and regression equation in the "Electric vehicle: mode*

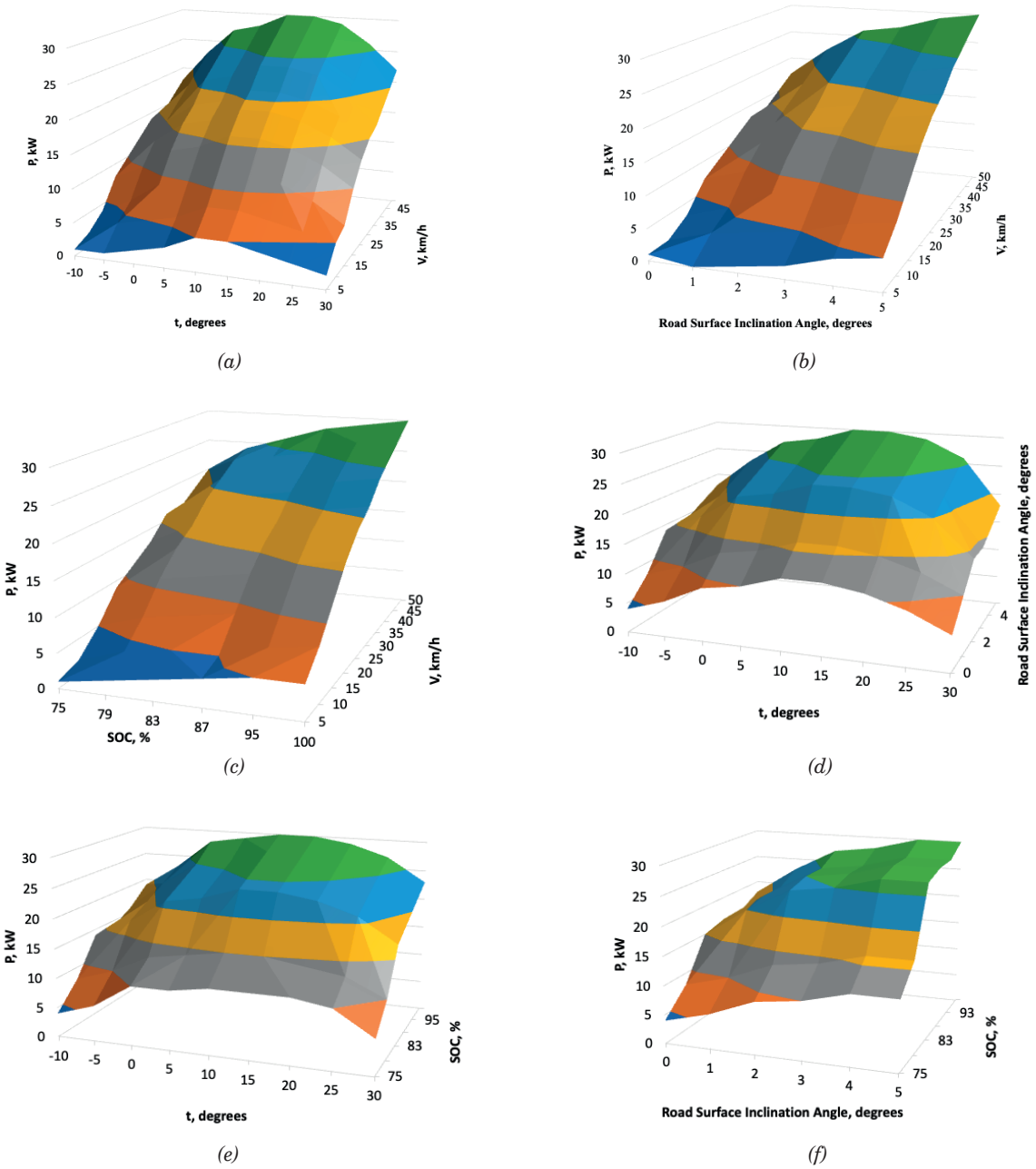

Figure 15 *Response surfaces of the model of specific power of a hybrid vehicle when factors change: a) "driving speed" and "environment t"; b) "driving speed" and "road surface angle"; c) "driving speed" and "SOC"; d) "environment t" and "road surface angle"; d) " environment t" and "SOC"; e) "road surface slope angle" and "SOC"*

modelling of the specific power of the hybrid in the "Electric vehicle" mode are shown in Table 6.

Based on the results of the experiment and the regression equation for different modes of operation of the hybrid installation (Figure 14), the difference between the values of specific power is 4 to 11%. The above mentioned indicates the adequacy of the results obtained.

To determine the nature of the influence of the selected performance indicators on the value of the specific power of a hybrid vehicle, the response surfaces of the model were developed with the alternate fixation of two factors at zero level and the change of two other factors (Figure 15).

Having analyzed the regression Equation (28) and the response surfaces of the model, the nature of the influence of the hybrid vehicle's performance on the change in specific power was determined. If the value of such factors as "driving speed", "road surface slope angle", and "SOC" (the regression coefficients of these factors have a positive sign) increases and the value of the factor "environment *t*" (the regression coefficient of the factor has a negative sign) decreases, the value of specific power *P* increases, as well. If the values of the above factors change in the opposite direction, the value of the specific power, on the contrary, would approach the minimum value.

Additionally, the transition from normalized to non-normalized factors was performed by the inverse transformation according to Equation (17) to obtain a polynomial model of the specific power of a hybrid vehicle suitable for use in forecasting tasks. After performing the transformation, an expression is deduced:

$$P = 0.53476 + 0.0621 \cdot x_1 + 0.0676 \cdot x_3 + \\ + 0.0545 \cdot x_4 - 0.0373 \cdot x_2^2. \quad (29)$$

The obtained polynomial models of the specific power of a hybrid vehicle with normalized and non-normalized factors, can be used as a basis for developing an automated system for monitoring the electric part of a hybrid vehicle. Additionally, these models can be used to estimate and predict the energy consumption of the electric part of the hybrid, as well as the vehicle range in the traction battery mode. Thus, the values of factors should be substantiated into the model in Equation (29); and the predicted value P can be applied to calculate the energy consumption of a hybrid vehicle and estimate the range of a trip in the battery mode. Additionally, based on a real data obtained during the vehicle operation, the model can be further adjusted to improve its accuracy and reliability.

4 Conclusion

A mathematical model and an algorithm for optimizing the operation of HPP (hybrid power plant), implemented in the MATLAB/Simulink environment, are considered in the paper. To assess the influence of energy and traction-speed parameters on the specific power of a hybrid vehicle, a regression equation was deduced by conducting a full factorial experiment. Based on the regression equation, the nature of the influence of HPP operational parameters on the change in the specific power of the unit is determined.

Having analyzed the values of the coefficients of the regression equation terms, a list of factors that greatly influence the change in the specific power of the vehicle with HPP was obtained. Therefore, the impact of operational factors on the specific power of a hybrid vehicle could be evaluated. This fact in turn can influence the acceleration and overall dynamic performance of a vehicle, as well as its overall efficiency and economy, and can significantly improve the driving range of a hybrid on a single battery charge. Adequacy of the developed mathematical model for determining the energy and traction-speed indicators of the vehicle movement with HPP was confirmed with a discrepancy of results within 4 to 11% in driving modes under the electric motor operation.

Acknowledgment

The authors received no financial support for the research, authorship and/or publication of this article.

Conflicts of interest

The authors declare that they have no known competing financial interests or personal relationships that could have appeared to influence the work reported in this paper.

References

[1] KUSZNIER, J. Influence of environmental factors on the intelligent management of photovoltaic and wind sections in a hybrid power plant. *Energies* [online]. 2023, **16**, 1716. eISSN 1996-1073. Available from: https://doi.org/10.3390/en16041716

[2] MORENO-GAMBOA, F., ESCUDERO-ATEHORTUA, A., NIETO-LONDONO, C. Alternatives to improve performance and operation of a hybrid solar thermal power plant using hybrid closed Brayton cycle. *Sustainability* [online]. 2022, **14**, 9479. eISSN 2071-1050. Available from: https://doi.org/10.3390/su14159479

[3] YALCIN S, HERDEM, M. S. Optimizing EV battery management: advanced hybrid reinforcement learning models for efficient charging and discharging. *Energies* [online]. 2024, **17**(12), 2883. eISSN 1996-1073. Available from: https://doi.org/10.3390/en17122883

[4] KESEEV, V. P. Gap analysis in eco categories, electric vehicle comparison and solutions to global transport challenges. *Communications - Scientific Letters of the University of Zilina* [online]. 2023, **25**(1), p. B34-B44. ISSN 1335-4205, eISSN 2585-7878. Available from: https://doi.org/10.26552/com.C.2023.008

[5] SANJARBEK, R., MAVLONOV, J., MUKHITDINOV, A. Analysis of the powertrain component size of electrified vehicles commercially available on the market. *Communications - Scientific Letters of the University of Zilina* [online]. 2024, **24**(1), p. B74-B86. ISSN 1335-4205, eISSN 2585-7878. Available from: https://doi.org/10.26552/com.C.2022.1.B74-B86

[6] SIMCAK, J., FRIVALDSKY, M., RESUTIK, P. The power analysis of semiconductor devices in multi-phase traction inverter topologies applicable in the automotive industry. *Communications - Scientific Letters of the University of Zilina* [online]. 2024, **26**(3), p. C21-C38. ISSN 1335-4205, eISSN 2585-7878. Available from: https://doi.org/10.26552/com.C.2024.034

[7] GAO, D. W., MI, C., EMADI. A. Modelling and simulation of electric and hybrid vehicles. *Proceedings of the IEEE* [online]. 2006, **95**(4), p. 729-745. ISSN 0018-9219, eISSN 1558-2256. Available from: https://doi.org/10.1109/JPROC.2006.890127

[8] LIN, C. C., FILIPI, Z., WANG, Y., LOUCA, L., PENG, H., ASSANIS, D., STEIN, J. Integrated feed-forward hybrid electric vehicle simulation in Simulink and its use for power management studies. SAE Technical Paper 2001-01-1334. 2001 Available from: https://doi.org/10.4271/2001-01-1334

[9] GAO, W. Performance comparison of a hybrid fuel cell-battery powertrain and a hybrid fuel cell-ultracapacitor powertrain. *IEEE Transactions on Vehicular Technology* [online]. 2005, **54**(3), p. 846-855. ISSN 0018-9545, eISSN 1939-9359. Available from: https://doi.org/10.1109/TVT.2005.847229

[10] GAO, W., PORANDLA. S. Design optimization of a parallel hybrid electric powertrain. In: 2005 IEEE Vehicle Power and Propulsion Conference [online]. IEEE. 2005. ISBN 0-7803-9280-9, ISSN 1938-8756, p. 530-535. Available from: https://doi.org/10.1109/VPPC.2005.1554609

[11] ONODA, S., EMADI. A. PSIM-based modelling of automotive power systems: conventional electric and hybrid electric vehicles. *IEEE Transactions on Vehicular Technology* [online]. 2004, **53**(2), p. 390-400. ISSN 0018-9545, eISSN 1939-9359. Available from: https://doi.org/10.1109/TVT.2004.823500

[12] JIANG, B.-H., HSU, C.-C., SU, N.-W., LIN, C.-C. A review of modern electric vehicle innovations for energy transition. *Energies* [online]. 2024; **17**(12), 2906. eISSN 1996-1073. Available from: https://doi.org/10.3390/en17122906

[13] ZARIPOV, R. Y., GAVRILOV, P., KARKU, A. D., SERIKPAEV, T. M. Ways to reduce the toxicity of diesel exhaust gases / Sposoby snijenia toksıchnosti vyhlopnyh gazov dizelnogo topliva [in Russian]. *Nauka i tekhnika Kazakhstana / Science and technology of Kazakhstan*. 2019, **1**, p. 75-84. ISSN 2788-8770.

[14] SHARMA, D., JIBHAKATE, LONARE, P. G., SAH, T., B. M., PANDEY, R. Study and modelling of hybrid MILD vehicle. *International Journal for Scientific Research and Development*. 2015, **3**(01), p. 272-274. ISSN 2321-0613.

[15] ALAMATSAZ, K, QUESNEL, F, EICKER, U. Enhancing electric shuttle bus efficiency: a case study on timetabling and scheduling optimization. *Energies* [online]. 2024, **17**(13), 3149. eISSN 1996-1073. Available from: https://doi.org/10.3390/en17133149

[16] YAN, X., ZHANG, H., LI, X., LI, Y., XU, L. Control strategy of torque distribution for hybrid four-wheel drive tractor. *World Electric Vehicle Journal* [online]. 2023, **14**, 190. eISSN 2032-6653. Available from: https://doi.org/10.3390/wevj14070190

[17] CHENG, R., DONG, Z. Modelling and simulation of plug-in hybrid electric powertrain system for different vehicular application. In: 2015 IEEE Vehicle Power and Propulsion Conference (VPPC): proceedings [online]. IEEE. 2015. eISBN 978-1-4673-7637-2. Available from: https://doi. org/10.1109/vppc.2015.7352976

[18] ADACHI, S., YOSHIDA, S., MIYATA, H., KOUGE, T., INOUE, D., TAKAMIYA, Y., NAGAUNE, F., KOBAYASHI, H., HEINZEL, T., NISHIURA, A. Automotive power module technologies for high-speed switching. In: International Exhibition and Conference for Power Electronics, Intelligent Motion, Renewable Energy and Energy Management: proceedings. 2016. p 1-7.

[19] DHAWAN, R., GUPTA, S., HENSLEY, R., HUDDAR, N., IYER, B., MANGALESWARAN, R. The future of mobility in India: challenges and opportunities for the auto component industry [online]. Available from: https://www.mckinsey.com/industries/automotive-and-assembly/our-insights/the-future-of-mobility-in-india-challenges-and-opportunities-for-the-auto-component-industry#/

[20] SINGH, S. Global electric vehicle market looks to power up in 2018 - Forbes [online], Available from: https://www.forbes.com/sites/sarwantsingh/2018/04/03/global-electric-vehicle-market-looks-to-fire-on-all-motors-in-2018/

[21] CHEN, H., SONG, Z., ZHAO, X., ZHANG, T., PEI, P., LIANG, CH. A review of durability test protocols of the proton exchange membrane fuel cells for vehicle. *Applied Energy* [online]. 2018, **224**, p. 289-299. ISSN 0306-2619, eISSN 1872-9118. Available from: https://doi.org/10.1016/j.apenergy.2018.04.050

[22] TARNAPOWICZ, D., GERMAN-GALKIN, S., NERC, A., JASKIEWICZ, M. Improving the energy efficiency of a ship's power plant by using an autonomous hybrid system with a PMSG. *Energies* [online]. 2023, **16**, 3158. eISSN 1996-1073. Available from: https://doi.org/10.3390/en16073158

[23] AULIN, V., ROGOVSKII, I., LYASHUK, O., TITOVA, L., HRYNKIV, A., MIRONOV, D., VOLIANSKYI, M., ROGATYNSKYI, R., SOLOMKA, O., LYSENKO, S. Comprehensive assessment of technical condition of vehicles during operation based on Harrington's desirability function. *Eastern-European Journal of Enterprise Technologies* [online]. 2024, **1**(3(127), p. 37-46. ISSN 1729-3774, eISSN 1729-4061. Available from: https://doi.org/10.15587/1729-4061.2024.298567

[24] O'KEEFE, R., ROACH, J. W. Artificial intelligence approach to simulation. *Journal of the Operational Research Society* [online]. 1987, **38**, p. 713-722. ISSN 0160-5682, eISSN 1476-9360. Available from: https://doi.org/10.2307/2582843

[25] MILLS, K. L., FILLIBEN, J. J., HAINES, A. L. Determining relative importance and effective settings for genetic algorithm control parameters. *Evolutionary Computation* [online]. 2015, **23**(2), p. 309-342. ISSN 1063-6560, eISSN 1530-9304. Available from: http://dx.doi.org/10.1162/EVCO_a_00137

[26] MIRONOV, D., LYASHUK, O., HEVKO, I., HUPKA, A., SLOBODIAN, L., HEVKO, B., KHOROSHUN, R. Development of a model of a generalized diagnostic indicator of the technical condition of the vehicle chassis using mathematical methods of the theory of experiment planning. *Advances in Mechanical Engineering and Transport* [online]. 2023, **2**(21), p. 135-144. ISSN 2313-5425. Available from: https://doi.org/10.36910/automash.v2i21.1218

[27] EN 1986-2:2001. Electrically propelled road vehicles. Measurement of energy performances. Part 2: Thermal electric hybrid vehicle. Brussels, Belgium: European Standard for Electrically Propelled Vehicles, 2001.

[28] EN 1986-1:1997. Electrically propelled road vehicles. Measurement of energy performances. Part 1: Pure electric vehicle. Brussels, Belgium: European Standard for Electrically Propelled Vehicles, 1997.